Bull. Mater. Sci. (2020) 43:36
https://doi.org/10.1007/s12034-019-2000-4

Crystallization and kinetics studies of $Ti_{20}Zr_{20}Cu_{60-x}Ni_x$ (x = 10, 20, 30 and 40) metallic glasses

P RAMA RAO[1,4,*], ANIL K BHATNAGAR[2] and BHASKAR MAJUMDAR[3]
[1]School of Engineering Sciences and Technology, University of Hyderabad, Hyderabad 500046, India
[2]School of Physics, University of Hyderabad, Hyderabad 50046, India
[3]Defence Metallurgical Research Laboratory (DMRL), Kanchanbagh, Hyderabad 500 058, India
[4]CSIR-Central Glass and Ceramic Research Institute, Kolkata 700032, India
*Author for correspondence (panugothu.ramarao@gmail.com)

MS received 26 September 2018; accepted 7 August 2019

Abstract. Synthesis and characterization of $Ti_{20}Zr_{20}Cu_{60-x}Ni_x$ (x = 10, 20, 30 and 40) metallic glasses are reported in this paper. Glassy ribbons are produced by rapid quenching using the standard copper wheel roller technique in argon atmosphere. Their structural characterization is carried out by X-ray diffraction (XRD) and thermal behaviour (crystallization) study by differential scanning calorimetry (DSC). Results of XRD on both sides of each ribbon sample confirmed that each sample was indeed amorphous/glassy as only a very broad peak in XRD pattern was observed. Metallic glass $Ti_{20}Zr_{20}Cu_{50}Ni_{10}$ shows three crystallization peaks in non-isothermal DSC scans while other three samples show only a single crystallization peak. The activation energy of crystallization for each sample has been calculated using three available models, namely, those of Kissinger, Augis–Bennett and Ozawa. All the three models gave nearly similar activation energies for a given sample within 10%.

Keywords. Amorphous alloys; metallic glasses; crystallization; activation energy.

1. Introduction

Metallic glasses of various compositions have been prepared since a few decades in the ribbon form and their use is well documented in various engineering applications [1–5]. However, now it is established that a number of complex alloys in the bulk form can be prepared in the glassy state using conventional ingot casting method by rapid quenching. These complex alloys may contain some of Ti, Zr, Hf, Mg, La, Cu, Fe, Ni, Pd and Pt metals. Ti-based bulk metallic glasses (BMGs) have been prepared and have received much attention as they seem to be important materials, which could be used for structural components for various applications as they are of relatively low weight and have high strength [6,7]. Many of these Ti-based metallic glasses show good glass-forming ability and superior mechanical properties but have low ductility [8–10]. Some of these alloys are being used for brazing purposes as the glassy/amorphous nature seems to accelerate atomic diffusion and surface reaction at high temperatures required for brazing. Further, the brazing temperatures normally are lower for glassy materials than those for polycrystalline materials. With a view to produce a Ti-based metallic glass system, which could be used to braze joints with Ti-alloy, we have prepared Ti–Zr–Cu–Ni-based metallic glasses in ribbon form and studied their properties and brazing effectiveness [11–15]. In this paper we report preparation and characterization of $Ti_{20}Zr_{20}Cu_{60-x}Ni_x$ (x = 10, 20, 30 and 40) by X-ray and differential scanning calorimetry (DSC) to study thermal stability. Other properties and brazing results will be presented in later papers.

2. Experimental

Amorphous ribbons of $Ti_{20}Zr_{20}Cu_{60-x}Ni_x$ (x= 10, 20, 30 and 40) alloys were prepared by a single-roller melt-spinning technique in an argon gas atmosphere. Ingots of polycrystalline alloys were prepared by induction melting of 99.99% pure Ti, 99.8% pure Zr, 99.999% pure Cu and 99.97% pure Ni on a water-cooled copper boat in a Ti-gettered argon atmosphere. The weight loss of each sample was less than 0.1% during the alloying process. Thus, the compositions of the alloys did not change significantly after melting. The alloy ingots were then re-melted in vacuum in a quartz tube using an RF induction coil and then injected into a rotating copper wheel in pure argon at about 1 atm pressure, producing thick ribbons of approximately 1 cm width and about 50 μm thicknesses. The crystalline/amorphous nature of the ribbons was examined by X-ray diffraction (XRD) using a Bruker Model NoD8 X-ray machine with Cu Kα radiation source (λ = 15.4 nm). The X-ray tube was operated at 45 kV and 40 mA in a step-scan mode with a step width of 0.035° and a sampling time of 7 s per step. The thermal behaviour of each sample was investigated using a Differential Scanning Calorimeter, Model 821

Published online: 19 December 2019

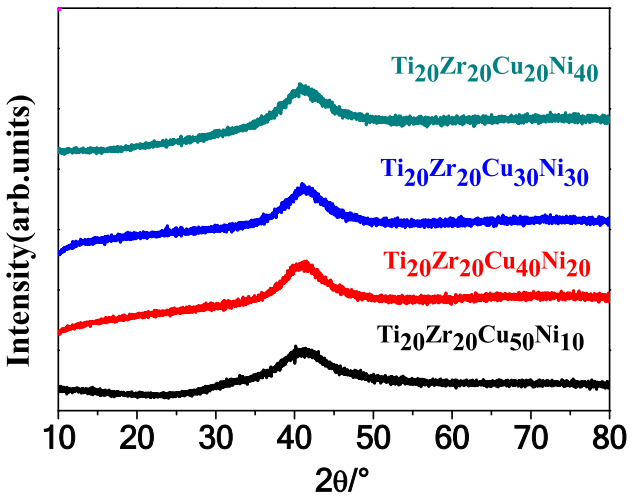

Figure 1. XRD spectra of the $Ti_{20}Zr_{20}Cu_{60-x}Ni_x$ (x = 10, 20, 30 and 40) metallic glasses.

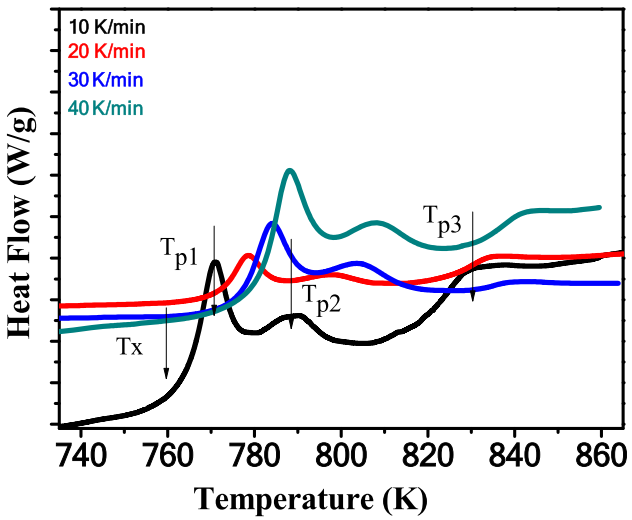

Figure 2. DSC thermograms of $Ti_{20}Zr_{20}Cu_{50}Ni_{10}$ metallic glass at different heating rates.

of METTLER-Toledo make, using non-isothermal DSC runs (in Ar flow) between room temperature (RT) and 650°C. Four different heating rates, i.e., 10, 20, 30 and 40 K min^{-1}, were used for the DSC runs.

3. Results and discussion

The characterization of each sample was done by taking XRD pattern on both sides of the ribbon to determine whether it had a glassy structure or not. Crystallization studies were done using non-isothermal DSC runs. DSC results were analysed using some available theoretical models to obtain activation energies for each sample.

3.1 *XRD*

The XRD patterns of all the samples are shown in figure 1. As seen from figure 1, the XRD pattern of each sample shows a very broad peak and shows no sharp peak. This observation confirms that each sample is glassy or has glassy nature. A characteristic broad hump of nearly equal width over 2θ = 35−45° is observed for each sample, indicating that the short range order may be nearly the same for each sample.

3.2 *Thermal behaviour/DSC results*

Non-isothermal DSC runs were performed using four heating rates, as mentioned earlier. They were 10, 20, 30 and 40 K min^{-1}. Approximately 8–10 mg of each sample was used for each DSC run using aluminium pans. Argon gas was made to flow in the experimental chamber during each run. Figures 2, 3, 4 and 5 show the DSC thermograms for $Ti_{20}Zr_{20}Cu_{60-x}Ni_x$ (x = 10, 20, 30 and 40) metallic glass samples. These thermograms consist of an exothermic peak or multiple peaks depending on the crystallization behaviour.

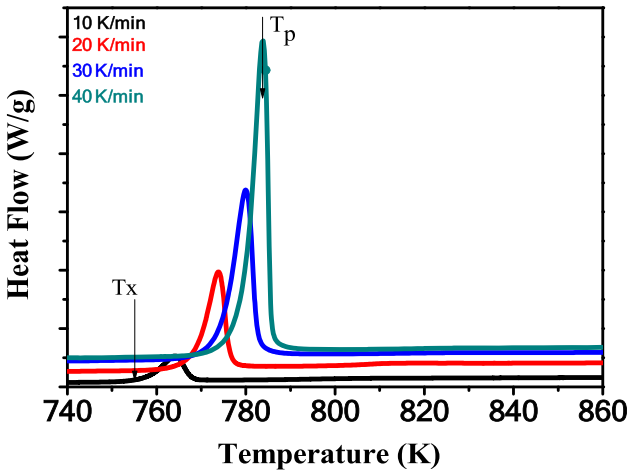

Figure 3. DSC thermograms of $Ti_{20}Zr_{20}Cu_{40}Ni_{20}$ metallic glass at different heating rates.

There was no observation of glass transition temperature for any of the samples within instrumental error, which is usually seen as a change in slope of the base line.

There are two characteristic temperatures involved in these runs. The temperature at which the crystallization process is initiated is denoted by T_x. This is determined by observing when the peak just starts evolving. The temperature at which the exothermic signal reaches maximum is denoted by T_p, the so-called peak temperature. Both of these two temperatures were clearly identifiable for all the heating rates. Figure 2 shows three exothermic peaks for x = 10 sample, the first one (lowest temperature) is sharper than the second one and the third peak is really broad. All other samples (x = 20−40) show only a single exothermic peak, which is much sharper than the first peak observed for x = 10. The results for x = 10

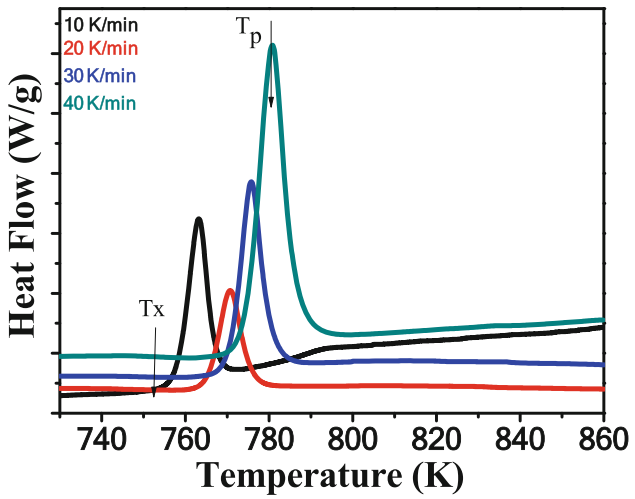

Figure 4. DSC thermograms of $Ti_{20}Zr_{20}Cu_{30}Ni_{30}$ metallic glass at different heating rates.

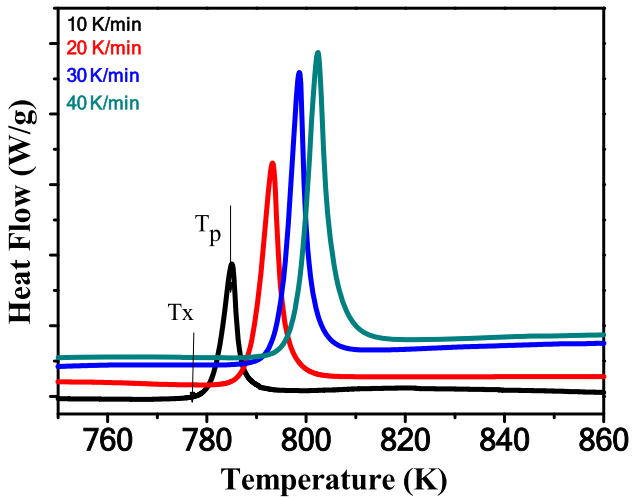

Figure 5. DSC thermograms of $Ti_{20}Zr_{20}Cu_{20}Ni_{40}$ metallic glass at different heating rates.

sample show that it has partial crystallization first, followed by second and third crystallization steps.

The second peak for $x = 10$ sample overlaps with the first peak (the end of first peak and the start of second peak), indicating that before the first step of the crystallization gets over, the second step of crystallization starts. The crystallization for all other samples takes place in one step and it is fast (the peak width is smaller; its FWHM is ∼4 K). Values of T_x and T_p for these samples are given in table 1, 2, 3 and 4. These temperatures have an accuracy of ±5 K except for the third peak for $x = 10$ sample, where error may be more as the peak is rather broad. It is observed that these temperatures increase with increase in the heating rate, which is normally observed for all metallic glasses.

The analysis result of the growth process of the first peak in figure 2 is slower than the observed for other samples,

Table 1. Variation of peak temperatures as a function of heating rate for $Ti_{20}Zr_{20}Cu_{50}Ni_{10}$ metallic glass.

	$Ti_{20}Zr_{20}Cu_{50}Ni_{10}$			
Heating rate (K min^{-1})	T_x (K)	T_{p1} (K)	T_{p2} (K)	T_{p3} (K)
10	755	771	789	831
20	771	778	798	835
30	775	784	803	840
40	780	788	807	842

Table 2. Variation of peak temperatures as a function of heating rate for $Ti_{20}Zr_{20}Cu_{40}Ni_{20}$ metallic glass.

	$Ti_{20}Zr_{20}Cu_{40}Ni_{20}$	
Heating rate (K min^{-1})	T_x (K)	T_P (K)
10	756	764
20	768	773
30	770	779
40	772	783

Table 3. Variation of peak temperatures as a function of heating rate for $Ti_{20}Zr_{20}Cu_{30}Ni_{30}$ metallic glass.

	$Ti_{20}Zr_{20}Cu_{30}Ni_{30}$	
Heating rate (K min^{-1})	T_x (K)	T_p (K)
10	757	763
20	764	770
30	767	775
40	771	780

Table 4. Variations of peak temperatures as a function of heating rate for $Ti_{20}Zr_{20}Cu_{20}Ni_{40}$ metallic glass.

	$Ti_{20}Zr_{20}Cu_{20}Ni_{40}$	
Heating rate (K min^{-1})	T_x (K)	T_p (K)
10	778	785
20	785	793
30	791	798
40	795	802

where the rise of the peak is relatively sharper. Multiple crystallization peaks have been observed in many metallic glasses. It simply shows that some of the elements in the glass form crystals during the first crystallization while some parts of the sample still remain in the glassy state. As the temperature increases, other components in the glass also crystallize. The first crystallization peak for $x = 10$ sample is relatively sharper than the second and third crystallization peaks,

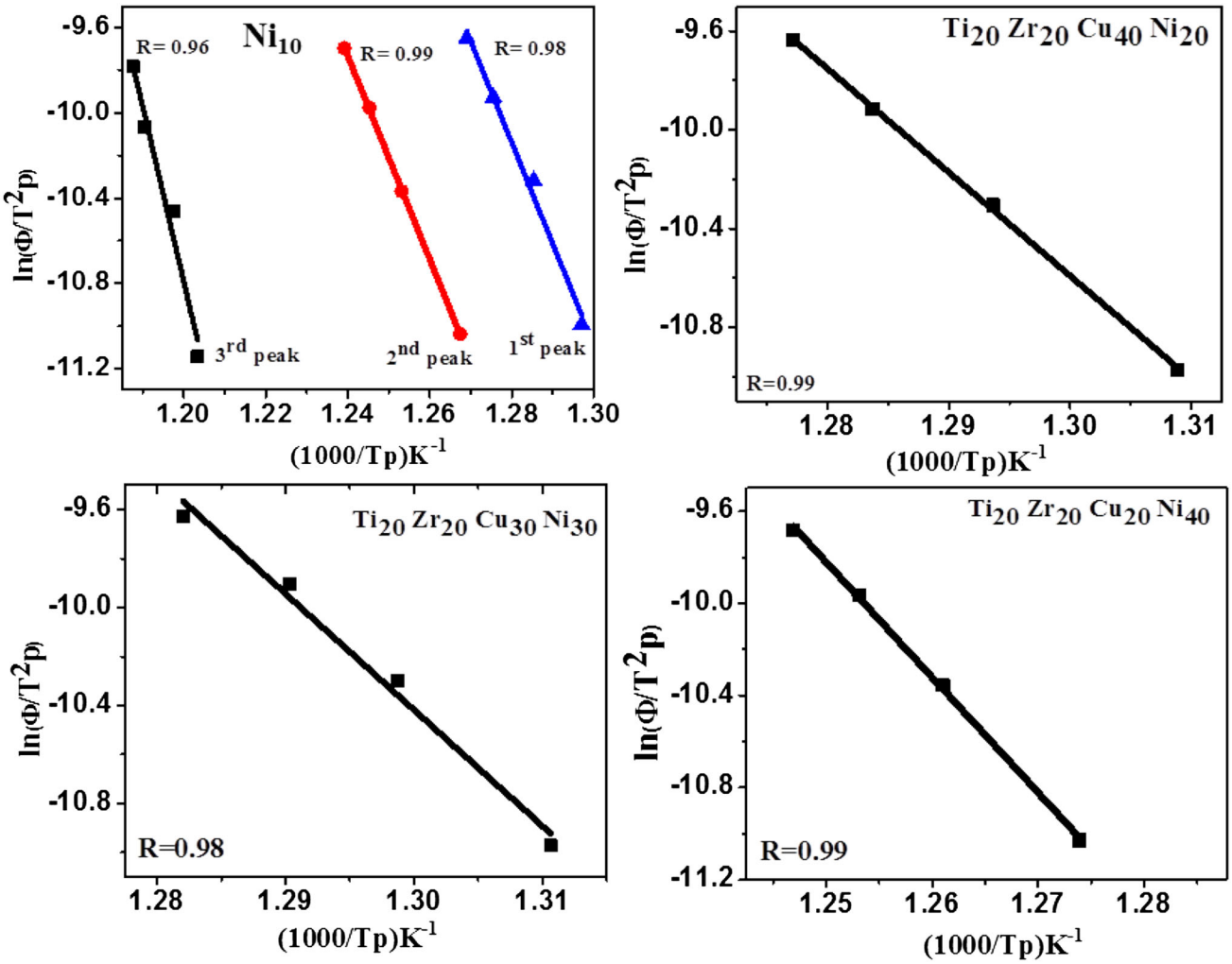

Figure 6. $\ln(O/T_p^2)$ *vs.* $(1000/T_p)$ of $Ti_{20}Zr_{20}Cu_{60-x}Ni_x$ (x = 10, 20, 30 and 40) metallic glasses for the first, second and third crystallization events.

which indicates the formation of nuclei and their growth at a relatively higher rate at the first peak when compared with other two peaks. Another observation is that for $x = 10$ sample, for the heating rate 10 K min^{-1}, $T_{p1} - T_x$ is 16 K, but for other heating rates it is ~8 K.

3.3 *Activation energy calculation*

Metallic glasses are in a metastable state; therefore, given enough energy, they tend to move to the lower energy state, that is, the crystallized state. The energy required to do this is termed as the activation energy. There are a number of models to calculate this energy. The most widely used and the oldest one is the Kissinger model [16]. Other models were proposed later. In the analysis of afore-mentioned DSC data, we have used three widely used models, namely, those proposed by Kissinger [16], Augis and Bennett [17] and Ozawa [18] to determine the activation energies and to see if there are large differences between the results or not.

3.3a *Kissinger model*: The most commonly used model to analyse the activation energy of both crystallization event and glass transition is the Kissinger model. According to this model, a homogeneous reaction follows the first-order rate equation given by

$$(dx/dt) = K(1 - x),$$

where x is the amount of a material transformed and K is a constant. Kissinger showed that the activation energy of such a transformation can be determined by DTA in different heating runs. Kissinger derived the following equation, which relates the heating rate, the peak temperature and the activation energy observed in DTA runs:

$$\ln(-\Phi/T_p^2) = -E_c/(RT_p) + \text{constant}, \quad (1)$$

where Φ is the heating rate, T_p is the peak temperature at heating rate Φ and E_c is the activation energy of the

Table 5. Activation energies (E_c) for crystallization of $Ti_{20}Zr_{20}Cu_{60-x}Ni_x$ (x = 10, 20, 30 and 40) metallic glasses (using Kissinger model).

	Activation energy for the crystallization process by Kissinger method (kJ mol^{-1})		
Composition	1st peak	2nd peak	3rd peak
$Ti_{20}Zr_{20}Cu_{50}Ni_{10}$	395	396	681
$Ti_{20}Zr_{20}Cu_{40}Ni_{20}$	349	—	—
$Ti_{20}Zr_{20}Cu_{30}Ni_{30}$	394	—	—
$Ti_{20}Zr_{20}Cu_{20}Ni_{40}$	416	—	—

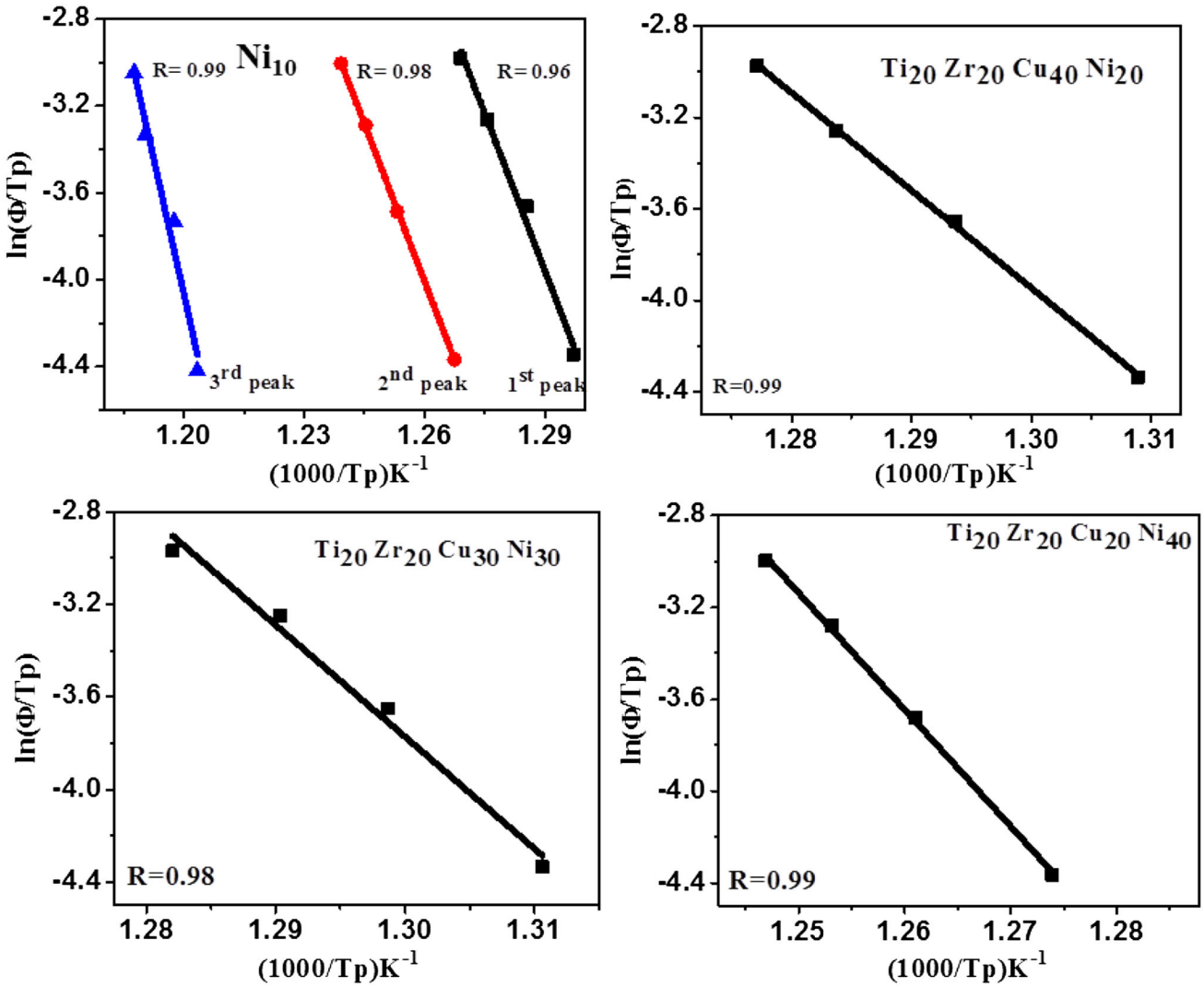

Figure 7. $\ln(O/T_p)$ *vs.* $(1000/T_p)$ of $Ti_{20}Zr_{20}Cu_{60-x}Ni_x$ (x = 10, 20, 30 and 40) metallic glasses.

reaction/transformation. The validity of this equation has been tested over the years and especially in case of crystallization of metallic glasses studied by both DTA and DSC. A plot of $\ln(-\Phi/T_p^2)$ *vs.* $1000/T_p$ should give a straight line. The slope of this straight line is equal to $(-E_c/R)$. Plots of $\ln(-\Phi/T_p^2)$ *vs.* $1000/T_p$ for all the samples are shown in figure 6. The best straight line fits of the experimental data to equation (1) for each sample are also shown in figure 6. The activation

Table 6. Activation energies (E_c) for crystallization of the $Ti_{20}Zr_{20}Cu_{60-x}Ni_x$ (x = 10, 20, 30 and 40) metallic glasses (from Augis and Bennett model).

	Activation energy for the crystallization process by Augis & Bennett method (kJ mol^{-1})		
Composition	1st peak	2nd peak	3nd peak
$Ti_{20}Zr_{20}Cu_{50}Ni_{10}$	401	403	688
$Ti_{20}Zr_{20}Cu_{40}Ni_{20}$	355	—	—
$Ti_{20}Zr_{20}Cu_{30}Ni_{30}$	401	—	—
$Ti_{20}Zr_{20}Cu_{20}Ni_{40}$	422	—	—

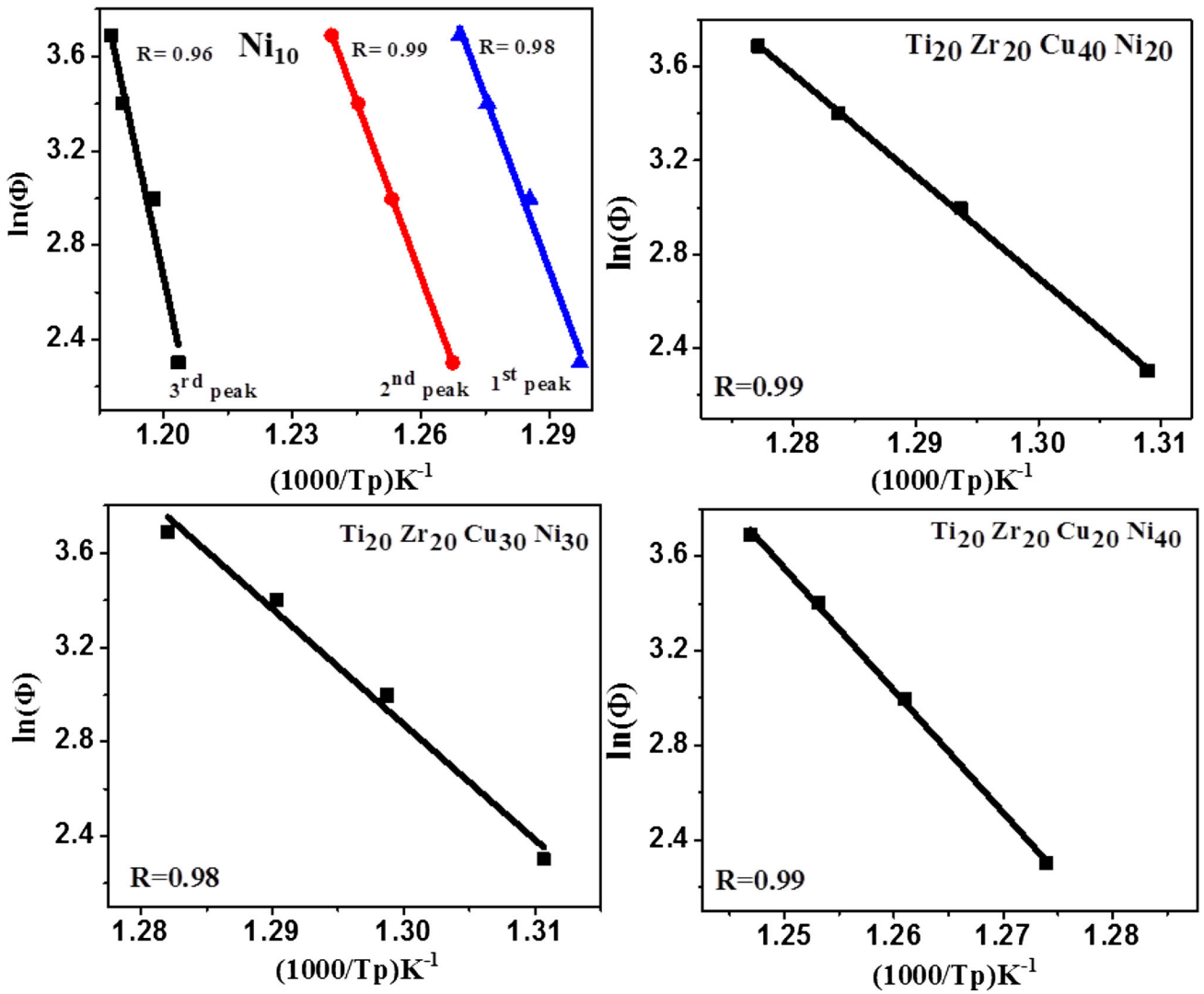

Figure 8. Plots of $\ln(O)$ *vs.* $(1000/T_p)$ of $Ti_{20}Zr_{20}Cu_{60-x}Ni_x$ (x = 10, 20, 30 and 40) metallic glasses.

energies for crystallizations for all the samples are evaluated from the slopes of these best fitted lines and they are presented in table 5. For $Ti_{20}Zr_{20}Cu_{50}Ni_{10}$ metallic glass the activation energies for the 1st, 2nd and 3rd peaks were calculated to be 395, 396 and 681 kJ mol^{-1}, respectively.

From table 5, it is observed that there is no systemic variation of the activation energy as a function of Ni in the samples. The activation energy for the first peak for $x = 10$ sample is higher than that of $x = 20$, and it increases for samples with $x = 20 - 40$.

Table 7. Activation energies (E_c) for crystallization of the $Ti_{20}Zr_{20}Cu_{60-x}Ni_x$ (x = 10, 20, 30 and 40) metallic glasses (from Ozawa model).

	Activation energy for the crystallization process by Ozawa method (kJ mol^{-1})		
Composition	1st peak	2nd peak	3nd peak
$Ti_{20}Zr_{20}Cu_{50}Ni_{10}$	408	410	695
$Ti_{20}Zr_{20}Cu_{40}Ni_{20}$	361	—	—
$Ti_{20}Zr_{20}Cu_{30}Ni_{30}$	407	—	—
$Ti_{20}Zr_{20}Cu_{20}Ni_{40}$	429	—	—

3.3b *Augis and Bennett model*: Kissinger's method or model to calculate activation energy assumes homogeneous reaction following first-order kinetics as explained earlier. Augis and Bennett [17] have extended the Kissinger's model applicable to heterogeneous reactions following the Avrami expression [19–21]:

$$x = 1 - \exp[(-kt)^n],$$

where n is a dimensionless exponent; k has the dimensions of reaction rate given by

$$k = K_o \exp(-E_c/RT),$$

where K_o is a constant (a frequency factor). Using this approach, they derived the following formula:

$$\ln[\Phi/(T_p - T_o)] = -(E_c/RT_p) + \text{constant},$$

where T_o is the initial temperature and the furnace temperature is varied as

$$T = T_o + \alpha t,$$

where t is the time. Since T_o is RT, it is much smaller than T_p; it is neglected and the Augis–Bennett expression is approximated to

$$\ln(\Phi/T_p) = -(E_c/RT_p) + \text{constant}.$$

This expression is used to plot $\ln(\Phi/T_p)$ *vs.* $1000/T_p$ for all the samples and these plots are shown in figure 7; $\ln(\Phi/T_p)$ *vs.* $1000/T_p$ data are fitted to a straight line. The slopes of the straight lines are used to calculate the activation energies for various samples, which are listed in table 6.

3.3c *Ozawa model*: Similarly, Ozawa modified the Kissinger method to obtain the following relation [18]:

$$\ln(\Phi) = -(E_c/RT_p) + \text{constant}.$$

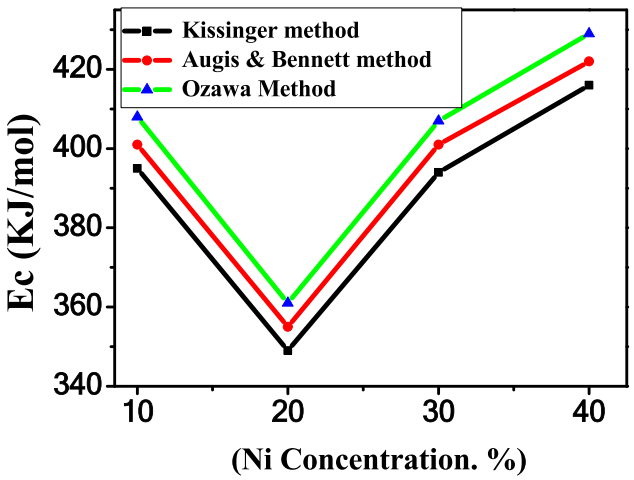

Figure 9. Plot of E_c values for the first peak obtained by various methods *vs.* Ni concentration %).

Thus, the experimental data, $\ln(\Phi)$ *vs.* $1000/T_p$, are plotted for all the samples, which are shown in figure 8. The data are best fitted to a straight line and the activation energies for all the samples are calculated using a procedure similar to that described earlier. These activation energies are listed in table 7.

It is observed that the activation energy for the first peak of $x = 10$ sample is higher than that for $x = 20$ sample in all the three models. It is also observed that all the three models give nearly the same (within a few percent) activation energy for a given sample. Therefore, it looks like one can use any of these three models. However, the Kissinger model has been widely used for calculating activation energies of metallic glasses.

Figure 9 shows activation energy plot *vs.* Ni concentration. It is observed that from $x = 20$ to $x = 40$, it is almost linear. Of course, the activation energy for $x = 10$ does not fall on this straight line [15]. The $x = 10$ sample behaviour is certainly different from those of other samples as it has three crystallization peaks while other samples have only one peak. One may have to look at the microstructure of these samples more carefully to figure out the reason for this deviation.

4. Conclusions

$Ti_{20}Zr_{20}Cu_{60-x}Ni_x$ (x = 10, 20, 30 and 40) samples were produced in the ribbon form by a rapid quenching technique. XRD on all the samples confirmed their glassy nature. The crystallization studies of $Ti_{20}Zr_{20}Cu_{60-x}Ni_x$ (x = 10, 20, 30 and 40) metallic glasses have been carried out by the non-isothermal DSC technique. Three theoretical models, proposed by Kissinger, Augis and Bennett, and Ozawa, have been used to analyse the DSC data to obtain activation energies of all the samples. The activation energies of these samples lie between ∼350 and 425 kJ mol^{-1}. The metallic glasses with x = 20, 30 and 40 show a single crystallization peak, while the one with $x = 10$ shows three crystallization peaks. The activation energy (E_c) for the first crystallization of $x = 10$ is observed to be higher than those for other samples. Activation energies for $x = 20, 30$ and 40 show almost a linear behaviour with x (Ni concentration).

Acknowledgements

We gratefully acknowledge the support of this research through the fund provided by the University Grants Commission-Rajiv Gandhi National Fellowship (UGC-RGNF). AKB thanks the Indian National Science Academy (INSA), New Delhi, for the support through Senior Scientist Platinum jubilee Fellowship. We would also like to express grateful thanks to Director, CSIR-CGCRI.

References

[1] Inoue A, Ohtera K, Kita K and Masumoto T 1988 *Jpn. J. Appl. Phys.* **27** L2248
[2] Inoue A, Zhang T and Masumoto T 1989 *Mater. Trans. JIM* **30** 965
[3] Inoue A, Zhang T and Masumoto T 1990 *Mater. Trans. JIM* **31** 177
[4] Peker A and Johnson W L 1993 *Appl. Phys. Lett.* **63** 2342
[5] Lin X H and Johnson W L 1995 *J. Appl. Phys.* **78** 6514
[6] Inoue A 1998 *Bulk amorphous alloys* (Zurich: Trans Tech Publications) p 1
[7] Spaepen F 1977 *Acta Metall.* **25** 407
[8] Kim J J, Choi Y, Suresh S and Argon A S 2002 *Science* **295** 654
[9] Wang W H, He D W, Zhao D Q, Yao Y S and He M 1999 *Appl. Phys. Lett.* **75** 2770
[10] Telford M 2004 *Mater. Today* **7** 36
[11] Zhang B, Zhao D Q, Pan M X, Wang W H and Greer A L 2005 *Phys. Rev. Lett.* **94** 205
[12] Martinez R, Kumar G and Schroers J 2008 *Scr. Mater.* **59** 187
[13] Chiu H M, Kumar G, Blawzdziewicz J and Schroers J 2009 *Scr. Mater.* **61** 28
[14] Schroers J, Hodges T M, Kumar G, Raman H, Barnes A J, Pham Q *et al* 2011 *Mater. Today* **14** 14
[15] Patel A T and Pratap A 2012 *J. Therm. Anal. Calorim.* **107** 159
[16] Kissinger H E 1956 *J. Res. Nat. Bur. Stand.* **57** 217
[17] Augis J A and Bennett J E 1978 *J. Therm. Anal.* **13** 283
[18] Ozawa T 1965 *Bull. Chem. Soc. Jpn.* **35** 1881
[19] Avrami M 1939 *J. Chem. Phys.* **7** 1103
[20] Avrami M 1940 *J. Chem. Phys.* **8** 212
[21] Avrami M 1941 *J. Chem. Phys.* **9** 177